Effect of nanosecond electromagnetic pulse (NEMP) irradiation amplitude on structure formation and properties of multicomponent Alx – Co – Cr – Fe – Ni system Alloys (x = 45–50 at.%) synthesized by SHS metallurgy

K. V. Doroshenko, *Post-Graduate Student, Department of Foundry and Metal Technology[1], e-mail: rbhbkk1212@yandex.ru*
Kh. Ri, *Doctor of Technical Sciences, Professor, Department of Foundry and Metal Technology[1], e-mail: opirus@bk.ru*
G. S. Dzuba, *Candidate of Technical Sciences, Associate Professor, Higher School of Industrial Engineering of the Polytechnic Institute[1], e-mail: 001012@pnu.edu.ru*
E. Kh. Ri, *Doctor of Technical Sciences, Professor, Head of Department of Foundry and Metal Technology[1], e-mail: erikri999@mail.ru*

[1]*Pacific National University, Khabarovsk, Russia.*

The influence of NEMP amplitude (0, 20, 30, 40 kV) on the processes of structure formation and liquation in the structural components of high-entropy alloys of the Al_x – Co – Cr –Fe – Ni system with different Al content (45, 47, 50 at.%) synthesized by SHS metallurgy has been investigated. The reacting mass was irradiated with NEMP to initiate SHS metallurgy, which was continued until complete solidification of the alloys. Electron scanning microscopy, micro-*X*-ray spectral analysis, and *X*-ray structural analysis were employed to study the process of alloy structure formation (x = 45–50 at.%), hardness, and microhardness tests were conducted in accordance with standard methods.
The regularities of changes in the structure of high-entropy alloys of the Al_x – Co – Cr – Fe – Ni system depending on the aluminum content and NEMP amplitude have been established. The presence of solid solutions of the studied alloys with different aluminum content and increasing amplitudes has been identified by micro-*X*-ray spectral analysis. The presence of complex-alloyed BCC (I) and BCC(II) solid solutions in the studied alloys is confirmed by the results of *X*-ray structural analysis.

Key words: alloy, structure formation, microhardness, multicomponent alloys, NEMP.
DOI: 10.17580/nfm.2025.01.06

Introduction

High entropy alloys are defined as those containing at least five elements, with concentrations ranging from 5 to 35 at.% [1, 2]. The high entropy of these alloys inhibits the formation of intermetallic compounds, allowing for the formation of simple face-centered cubic or volume-centered cubic structures [3, 4]. Additionally, the composition of the alloy can be altered to achieve desired properties.

High-entropy Al – Co – Cr – Fe – Ni alloys have been extensively studied for their compressibility, high hardness, high strength, corrosion resistance, and wear resistance. Wang et al. [5] observed that the AlCoCrFeNi alloy exhibited a dendritic BCC structure and exhibited excellent compressive properties, with an ultimate plastic strain of 32.7%. Sheng et al. [6] observed that the hardness of the $Al_{0.5}$CoCrFeCuNi alloy reached a maximum (252 HV) following annealing at 600 °C for 24 hours. Yen et al. [8] demonstrated that annealing enhances the corrosion resistance of the AlCoCrFeNi alloy. Munitz et al. [11] observed that the properties of the AlCoCrFeNi alloy undergo significant changes following heat treatment. Following annealing at 850 °C, the BCC phase underwent a transformation into the brittle σ-phase, accompanied by a sharp increase in microhardness of the dendrites, which subsequently transformed back at 975 °C. Following annealing at 1200 °C, the combination of softer dendritic regions and harder interdendritic regions resulted in a unique high compressive strength. As the research on equiatomic high-entropy AlCoCrFeNi alloys tends to be perfect, more and more studies are directed towards changing the composition of one or more elements. High-entropy Al_xCoCrFeNi alloys have been the subject of extensive investigation [12–16]. It has been demonstrated that the phase composition varies with Al content. Mohan et al. [13] observed that high-entropy Al_xCoCrFeNi (x = 0~1) alloys exhibited high stability when annealed at 400~800 °C. As the Al content increased, the volume fraction of the BCC phase increased, and the hardness also increased [13]. Li et al. [10] considered the phase in Al_xCoCrFeNi (x = 1~3) alloys to be B2 structure. The hardness of the alloys increases with increasing x value, with the highest hardness (740 HV) achieved at x = 3. Chuang et al. [9] demonstrated that the wear resistance of $Co_{1.5}CrFeNi_{1.5}Ti$ and $Al_{0.2}Co_{1.5}CrFeNi_{1.5}Ti$ alloys is at least twice that of conventional wear-resistant steels with similar hardness, due to their antioxidant properties and resistance. Joseph et al. [17] observed that $Al_{0.3}CoCrFeNi$ and $Al_{0.6}CoCrFeNi$ exhibited the lowest wear rate at 600 °C. Upon further heating, the wear rate of $Al_{0.6}CoCrFeNi$ increased, while that of $Al_{0.3}CoCrFeNi$ remained unchanged. This phenomenon can be attributed to the formation of a wear layer comprising fine particles with B2 release. Zhang et al. [18] observed that both the $AlCoCrFe_{1.5}Ni$ coating with B2 particles and the $AlCoCrFe_{2.5}Ni$ coating with BCC precipitates exhibited high strength, hardness, and wear resistance. Kang et al. [19] found that the high-entropy $AlCo_xCrFeNi$ alloy is composed of BCC and B2 phases. The addition of Co prevents the formation of the B2 phase. As the Co content increases, the hardness of the alloy decreases, while the compression characteristics improve. Qin et al. [20] reported that an increased Co content can initiate the formation of the FCC phase in high-entropy alloys $(AlCoCrFeNi)_{100-x}Co_x$. In high-entropy AlCoCrFeNi alloys, Al has been demonstrated to promote the formation of the B2 phase, as evidenced by numerous studies [7, 21–24] employing techniques such as atom probe tomography (APT), transmission electron microscopy (TEM), *X*-ray diffraction (XRD), and energy dispersive spectroscopy (EDS). Tan et al. [21] employed APT and TEM to distinguish the B2 phase from the BCC phase. The researchers discovered that BCC nanoprecipitates are enriched in Co, Cr, and Fe, while the B2 phase is enriched in Ni and Al. In general, the B2 phase exhibits greater hardness, while the FCC phase displays enhanced ductility, which collectively confers superior performance by regulating the ratio between the FCC phase and the B2 phase [18].

The authors studies have demonstrated the potential of NEMP as a modifier in the crystallization of alloys.

In light of these findings, it can be concluded that the development of alloys based on the Al_x – Co – Cr – Fe – Ni system with 45–50 at.% aluminum, synthesized by SHS metallurgy and irradiated with NEMP, is a promising area of research.

The objective of this study is to investigate the influence of NEMP (20, 30, 40 kV) irradiation of melts on the formation of structures, liquation processes, and properties of the alloy of the Al_x – Co – Cr – Fe – Ni system (x = 45–50 at.%) synthesized by SHS metallurgy.

Accordingly, the following objectives were set and subsequently addressed in this work:

1) The effect of NEMP (0, 20, 30, 40 kV) melt irradiation on the formation of structures and the character of element distribution in structural components of alloys with different aluminum content (45, 47, 50 at.%) will be investigated.

2) The structural components will be identified by micro-*X*-ray spectral and *X*-ray structural analysis.

3) An investigation was conducted to determine the hardness and microhardness of structural components as a function of aluminum content and the amplitude of NEMP irradiation (0, 20, 30, 40 kV).

Table 1
Initial charge components and aluminum content in the alloy (at.%)

Fractional parts of the charge components	Aluminum content in the alloy, at.%
$NiO : Co_2O_3 : Cr_2O_3 : Fe_2O_3 : Al = 5 : 5 : 5 : 5 : 10$	45
$NiO : Co_2O_3 : Cr_2O_3 : Fe_2O_3 : Al = 5 : 5 : 5 : 5 : 11$	47
$NiO : Co_2O_3 : Cr_2O_3 : Fe_2O_3 : Al = 5 : 5 : 5 : 5 : 12$	50

Materials and methods

The starting materials were NiO (99.5 wt.%), CoO (99.9 wt.%), Cr_2O_3 (99.9 wt.%), Fe_2O_3 (99 wt.%), calcium fluoride CaF_2 (98.0 wt.%), $NaNO_3$, and aluminum powder (98.0 wt.%). The **Table 1** below shows the compositions of the initial charge used in the synthesis and the content in at.% Al in the alloys.

The synthesis of high-entropy alloys was conducted in heat-resistant ceramic crucibles lined with refractory material. The charge preparation procedure involved processing in a planetary micromill PULVERISETTE 5 in an isopropyl alcohol medium, followed by drying in a vacuum drying cabinet SHS-90/B at a temperature of 80 °C.

The initial components were mixed in a certain stoichiometric ratio for 15 minutes until a homogeneous composition was achieved. The obtained mixture was then poured into the crucible. Prior to this, 200 mg of magnesium powder without additional oxidising agents was added as a fuse – initiator of combustion. At the irradiation of NEMP, there was sparking between the electrodes immersed to the bottom of the crucible in thermite mixtures, which led to the initiation of SHS metallurgy. In consideration of the abrasion losses incurred during milling, the mass of each sample was determined to be 63 ± 0.5 g. Following the ignition of the charge, a combustion front is distributed uniformly throughout the entire volume of the mixture. Subsequently, a layer of melt of combustion products is formed, comprising two distinct phases: metal and slag (Al_2O_3). Due to the disparity in specific gravity and mutual insolubility, phase separation occurs under the influence of gravity. As a consequence of heat exchange, the melt cools and crystallises at the conclusion of the process. As a result of the reaction, a two-layer product is formed: a compact metal ingot in the lower layer and an oxide slag in the upper layer, which can be readily separated from each other. A GIN-50-1NK generator was employed as a source of NEMP. The NEMP generator of the GIN-50-1NK type exhibits the following characteristics: a pulse duration of 4–6 ns, an amplitude of 50 kV, a power in one pulse exceeding 50 MW, a pulse repetition frequency of 1000 Hz, and a pulse electromagnetic field strength reaching up to 108 ... 1010 V/m.

A thermodynamic model was developed to investigate the phase formation of alloys within the Al – Co – Cr –

Fe – Ni system. This was achieved through the CALPHAD method, utilising the ThermoCalc(2023b) software package with the TCHEA 5.1 (HEA) database [26].

The following research methods were employed. A micro- *X*-ray spectral analysis was conducted to determine the content of elements in various structural components of alloys. This analysis was carried out on an analytical research complex based on FE-SEM Hitachi SU-70 (Japan) with energy dispersive (Thermo Scientific Ultra Dry) and wave (Thermo Scientific Magna Ray) attachments for micro-*X*-ray spectral analysis. The analytical research complex, based on FE-SEM Carl Zeiss Merlin (Germany), was utilized in conjunction with the reflected electron diffraction attachment, Instruments HKLN Nordlys. *X*-ray diffraction analysis was conducted on a diffractometer Dron 7, while microhardness (HV) testing was performed on a Shimadzu HMV-G21DT instrument.

Results and discussion

A computer simulation of the Al_xCoCrFeNi system (x = 20...55 at.%) was carried out in order to study the compositions of alloys with aluminum content up to 55 at.%. The results are presented in **Fig. 1.**

The composition of alloys corresponds to the 2-phase region, wherein the primary solidified phase is BCC (I) and a mixture of BCC (I) + BCC (II) is observed as the eutectic in the remaining liquid. The aluminum fraction is up to 45 at.%. At an aluminum fraction of approximately 45 atomic percent, BCC (I) solidifies initially, followed by a polymorphic transformation, BCC (I) → BCC (II). Chromium aluminides should then form a eutectic with the remaining liquid.

The structures of the synthesized alloys of the Al_x – Co – Cr – Fe – Ni system (x = 45, 47, and 50 at.% Al) were examined following irradiation with an amplitude ranging from 0 to 40 kV NEMP. NEMP irradiation was employed for the initiation of SHS metallurgy and the synthesis of multicomponent alloys prior to alloy crystallization. **Fig. 2** illustrate the microstructures of the investigated alloys in optical and scanning electron microscopes, respectively.

The formation of solid solutions in Al_xCoCrFeNi alloys was revealed upon irradiation of synthesized alloys containing 45, 47, and 50 at.% Al with amplituцdes of 20, 30, and 40 kV NEMP.

The average compositions of the alloys with 45, 47, and 50 at.% Al, irradiated with different amplitudes of NEMP, were obtained through micro-*X*-ray spectral analysis of points corresponding to the solid solution of light gray and dark gray BCC (I) and BCC (II).

Table 2 presents the mean compositions of alloys with 45 at.% Al subjected to varying NEMP amplitudes.

In the initial alloy with 45 at.% Al without NEMP, limited regions of BCC(I) solid solution of light gray color with variable chemical composition are observed. The light gray solid solution of BCC(I) type exhibits an increased content of Al, Ni, and Co and a decreased concentration of Cr, Fe in comparison to the dark gray solid solution of BCC(I) type.

Irradiation of the melt by NEMP with an amplitude of 20 kV results in a change in chemical composition that is consistent with the original character. The solid solution of BCC (I) of light gray color exhibits an increase in the dissolution of Al, Ni, and Co, while the dissolution of Cr and Fe is reduced. In contrast, the solid solution of BCC (I) of dark gray color displays a different dissolution pattern, with an increase in Cr and Fe dissolution and a reduction in Al, Ni, and Co dissolution.

A comparable pattern is observed when the melt is irradiated with an amplitude of 30 kV. The concentration of Al, Ni and Co is markedly higher in the solid solution of BCC (I) of light gray color, while the concentration of Cr and Fe is significantly lower, in comparison to the solid solution of BCC (I) of dark gray color.

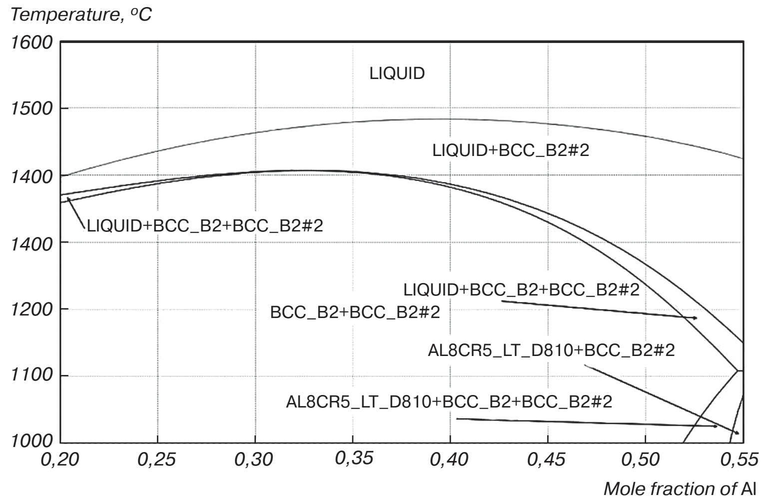

Fig. 1. Diagram of Al_xCoCrFeNi, x = 20...55 at.% in the temperature range from 1000 to 1500 °C

This phase composition change upon melt irradiation with an NEMP amplitude of 40 kV is maintained in both light gray and dark gray BCC (I) alloys.

As the NEMP amplitude increases from 0 to 40 kV (as illustrated in **Table 2** and **Fig. 3**), the aluminum content in the BCC (I) solid solutions of the two colors rises from 46.37 (42.87) at. The percentage of aluminum in the BCC (I) solid solutions of the two colors increases from 46.37 (42.87) at. to 52.29 (47.92) at. Percent. The aluminum content of the dark gray BCC (I) solid solution is provided in parentheses. The concentration of other elements also decreases:

– Ni from 14.05 (9.9) at. This represents a decrease from 14.05 (9.9) at.% to 13.55 (7.75) at.%;

– Chromium content decreased from 14.45 (22.95) at.%. The percentage decreases to 10.05 (22.41) at.%;

– Fe from 11.6 (14.09) at. The percentage decreased to 9.8 (13.4) at.%;

– Co from 13.53 (10.19) at.%. Following irradiation with an amplitude of 30 kV at NEMP, there was a further increase in concentration up to 14.3 at.%. The percentage of Co at an NEMP amplitude of 40 kV is as follows. Upon irradiation of the melt with NEMP at an amplitude of 40 kV, a BCC (II) solid solution was identified, containing in at. The composition of the solid solution was found to be 42.22% Al, 3.59% Ni, 36.95% Cr, 12.69% Fe, and 4.56% Co. It can be concluded that the high chromium content (36.95 at.%) and the lower concentration of Al, Ni, and Co compared to the solubility of similar elements in BCC (I) solid solutions with two types are the result of the dissolution of these elements in the solid solution. The content of Fe practically does not change.

Therefore, in alloys with 45 at.% Al without irradiation and with NEMP irradiation with amplitudes of 20 and 30 kV, two distinct types of BCC (I) solid solutions with varying chemical compositions are observed.

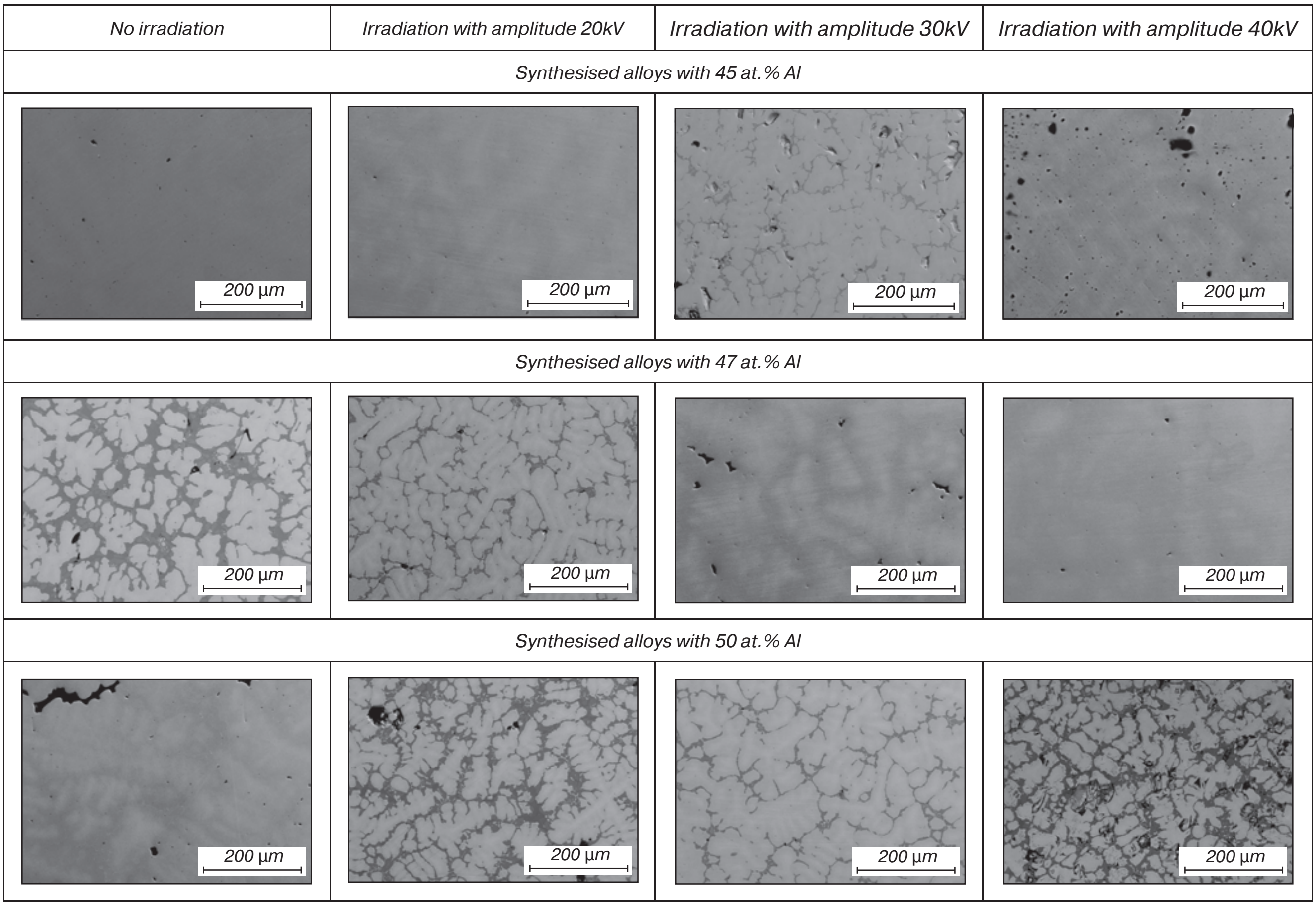

Fig. 2. Microstructures of synthesised alloys with 45–50 at.% Al irradiated with NEMP in reflected electrons on scanning electron microscope (SEM)

Table 2
Compositions of alloys with 45 at.% Al irradiated with different NEMP amplitudes

No.	NEMP amplitudes	Points of element analysis	Content of elements, at.%				
			Al	Ni	Cr	Fe	Co
1	0	BCC (I)-type solid solution of light gray color	46.37	14.05	14.45	11.6	13.53
		BCC (I)-type solid solution of dark gray color	42.87	9.9	22.95	14.09	10.19
2	20	BCC (I)-type solid solution of light gray color	47.29	13.92	13.58	11.67	13.54
		BCC (I)-type solid solution of dark gray color	43.97	7.47	26.99	13.94	7.64
3	30	BCC (I)-type solid solution of light gray color	49.55	12.24	14.14	11.42	12.66
		BCC (I)-type solid solution of dark gray color	47.09	8.48	22.63	12.76	9.06
4	40	BCC (II)-type solid solution	42.22	3.59	36.95	12.69	4.56
		BCC (I)-type solid solution of light gray color	52.29	13.55	10.05	9.8	14.3
		BCC (I)-type solid solution of dark gray color	47.92	7.75	22.41	13.4	8.53

Furthermore, when the melt is irradiated with NEMP with an amplitude of 40 kV, a third solid solution of BCC (II) is identified.

Table 3 illustrates the compositions of alloys with 50 at. % Al, which were not subjected to nor irradiated by NEMP with amplitudes of 20 and 40 kV.

In the absence of NEMP irradiation, the following phases undergo crystallization:

– The BCC (I) type solid solution is characterized by a light gray color and a composition of 51.05% Al, 16.47% Ni, 8.12% Cr, 9.06% Fe, and 15.3% Co in at.%.

– The BCC (I) solid solution exhibits a dark gray color and the following composition, in atomic percent: 49.24 Al; 10.8 Ni; 17.13 Cr; 12.5 Fe; 10.34 Co.

– The BCC type solid solution (II) has the following composition: 38.79 at.% Al, 2.55 at.% Ni, 43.87 at.% Cr, 11.65 at.% Fe, and 3.14 at.% Co.

Irradiation of the melt by NEMP with an amplitude of 20 kV resulted in the crystallization of the following phases:

– The BCC type solid solution (I) exhibits a light gray coloration and is composed of the following elements: 54.76% Al, 11.28% Ni, 12.52% Cr, 10.76% Fe, and 10.88% Co.

– The BCC (I) solid solution is characterized by a dark gray color and a composition of 68.16% Al, 6.35% Ni, 10.17% Cr, 9% Fe, and 6.33% Co in atomic percent.

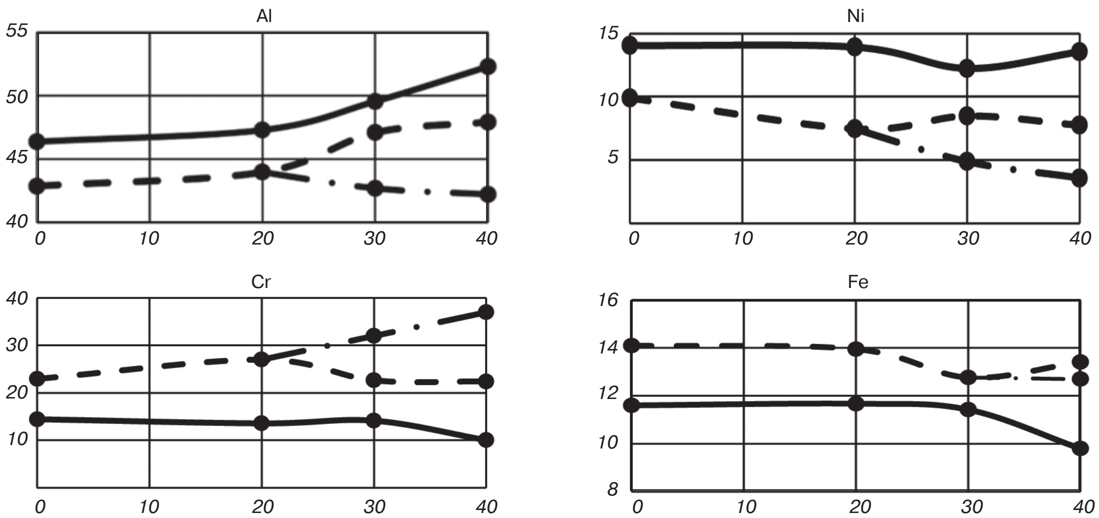

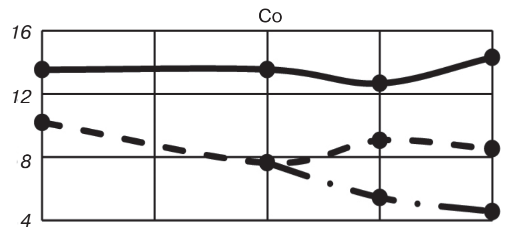

Fig. 3. Content of elements in solid solutions of BCC (I) type of light gray and dark gray shades and synthesized alloy with 45 at.% Al as a function of NEMP amplitude

Table 3
Compositions of alloys with 50 at. % Al irradiated with different NEMP amplitudes

№	NEMP amplitudes	Points of element analysis	Content of elements, at. %				
			Al	Ni	Cr	Fe	Co
1	0	BCC (II)-type solid solution	38.79	2.55	43.87	11.65	3.14
		BCC (I)-type solid solution of light gray color	51.05	16.47	8.12	9.06	15.3
		BCC (I)-type solid solution of dark gray color	49.24	10.8	17.13	12.5	10.34
2	20	BCC (I)-type solid solution of dark gray color	68.16	6.35	10.17	9.0	6.33
		BCC (II)-type solid solution	60.76	1.5	26.67	8.67	2.4
		BCC (I)-type solid solution of light gray color	54.76	11.28	12.52	10.76	10.88
		BCC (I)-type solid solution of dark gray color	54.29	10.66	13.55	11.07	10.43
		BCC (II)-type solid solution	59.66	1.18	28.24	8.72	2.2
3	40	BCC (II)-type solid solution	39.47	1.43	45.47	11.06	2.58
		BCC type solid solution (I) near white colored inclusions	48.9	9.22	19.96	13.17	8.76
		BCC (I)-type solid solution of light gray color	52.26	15.05	8.95	9.44	14.3

– The BCC type solid solution (II) has the following composition: 60.76% Al, 1.5% Ni, 26.67% Cr, 8.67% Fe, and 2.4% Co.

Upon irradiation of the melt by NEMP with an amplitude of 40 kV, the phases undergo crystallization.

The BCC type solid solution (I) is characterized by a light gray color and a composition of the following elements, in atomic percentage: 52.26 Al; 15.05 Ni; 8.25 Cr; 9.44 Fe; 10.88 Co.

The BCC (I) solid solution is of a dark gray color and has the following composition (in at.%): 48.9 Al; 9.22 Ni; 19.96 Cr; 13.17 Fe; 8.76 Co.

As illustrated in **Table 3** and **Fig. 4**, the content of Al, Fe, and Cr exhibits a pronounced variation with increasing amplitude from 0 to 40 kV. This variation is characterized by maxima when the melt is treated with an NEMP amplitude of 30 kV, while the concentration of Ni and Co also displays a notable dependence, albeit with minima in the Al content.

The content of the BCC (II) solid solution varies in accordance with the extreme dependence on the NEMP amplitude, exhibiting a maximum at an amplitude of 20 kV and minima for the other elements, namely Ni, Cr, Fe, and Co. The dissolution of Al, Ni, and Co in the BCC (II) solid solution is less extensive than that observed in the BCC (1) solid solution. Conversely, the content of Fe remains practically unchanged.

Therefore, the distribution of elements in the structural components of the Al_x – Co – Cr – Fe – Ni alloy subjected to NEMP melt irradiation differs significantly from that observed in alloys with an aluminum content of 45 at.% Al.

One may hypothesize that when nanosecond electromagnetic current pulses are introduced into the melt, electromagnetic fields with high intensity may be generated at specific moments. These electromagnetic fields result in the redistribution of elements within BCC (I) and BCC (II) solid solutions, leading to alterations in their structures and alloy properties. This phenomenon is likely the primary cause of the variation in element composition observed in the solid solutions of BCC (I) dark gray and light gray shaded alloys and BCC (II) subjected to an amplitude of 20–30 kV NEMP irradiation.

The discrepancy between the compositions of the experimental alloys and those obtained through computer modeling can be attributed to the high cooling rate of the synthesized multicomponent alloys during the crystallization of the metal ingot.

Fig. 5 shows the *X*-ray diffraction patterns of alloys with 45 and 50 at.% Al irradiated with different NEMP amplitudes during their synthesis by SHS metallurgy.

The obtained results of *X*-ray phase analysis allow us to conclude that:

– the alloy with 45 at.% Al without irradiation and with irradiation up to 30 kV NEMP is a BCC solid solution, and

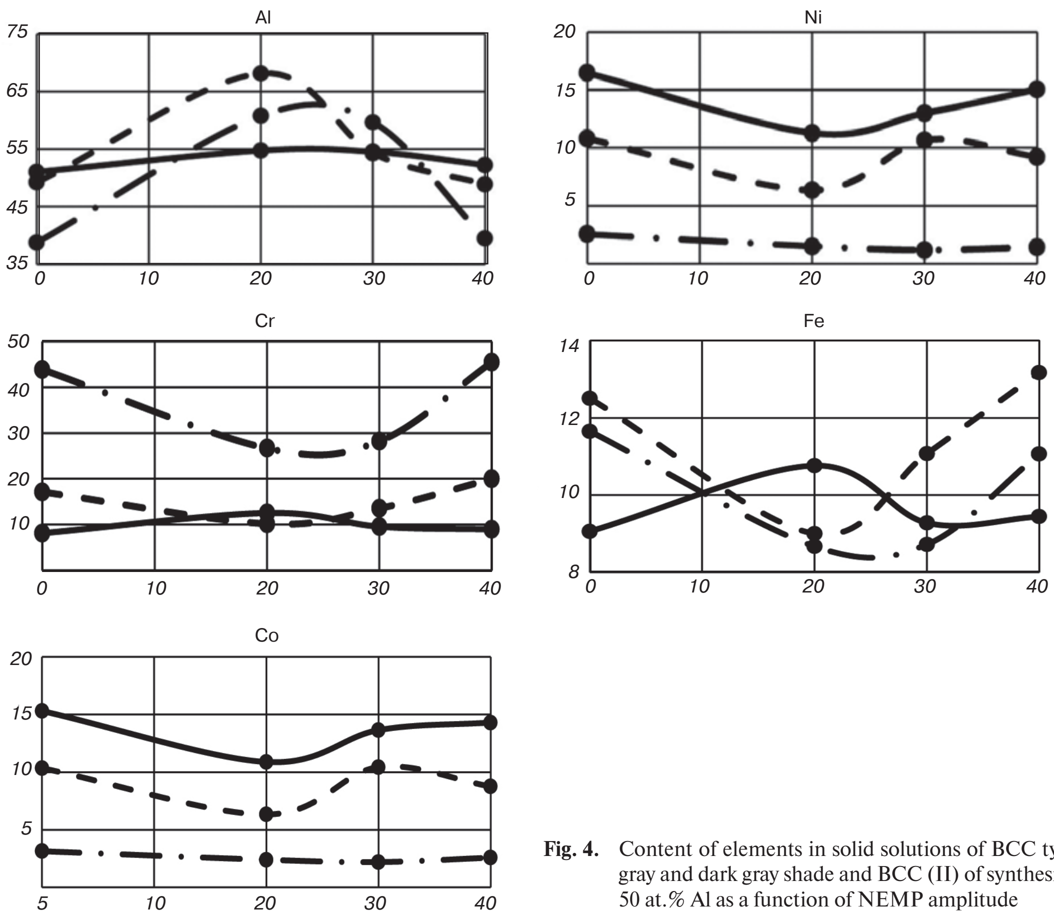

Fig. 4. Content of elements in solid solutions of BCC type (I) of light gray and dark gray shade and BCC (II) of synthesized alloy with 50 at.% Al as a function of NEMP amplitude

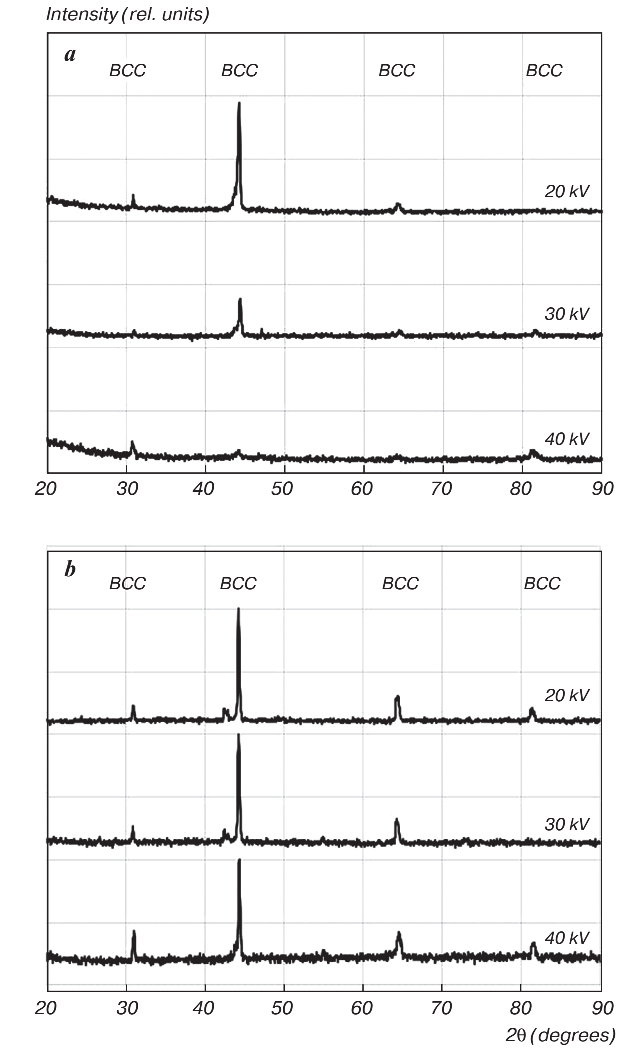

Fig. 5. *X*-ray diffraction patterns of synthesized alloys with 45 and 50 at.% Al irradiated with 20, 30, 40 kV NEMP amplitude: *a* – 45 at.% Al, *b* – 50 at.% Al

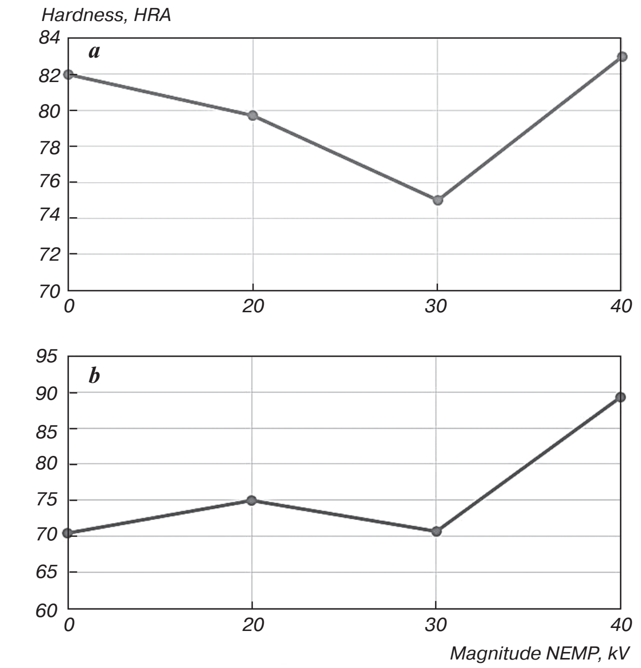

Fig. 6. Effect of NEMP amplitude on the hardness of the synthesized alloy:
` *a* – 45 at.% Al, *b* – 50 at.% Al

at 40 kV NEMP irradiation it was not possible to identify the peaks of BCC solid solution;

– alloy with 50 at. % Al with and without NEMP irradiation is a BCC solid solution.

In this work, the effect of NEMP amplitude on hardness **(Fig. 6)** and microhardness of BCC (I) solid solutions in light gray and dark gray shaded regions **(Fig. 7)** of synthesized alloys with 45 and 50 at.% Al was investigated.

As illustrated in **Fig. 6**, the dependences exhibit maxima and minima. In the alloy with 45 at. % Al at 30 kV NEMP irradiation, the hardness reaches a minimum (75 HRA) (without irradiation, 82 HRA). In the alloy with 50 at.% Al at irradiation, the hardness value increases with a maximum at 40 kV NEMP, reaching approximately 90 HRA (without irradiation, 70 HRA).

Fig. 7 illustrates the correlation between microhardness and NEMP amplitude (0–40 kV) for light gray and dark gray BCC (I) solid solutions and BCC (II) alloys with 45 and 50 at.% Al.

The results of the experiments yielded the following findings:

– In alloys with 45 at.% Al and an increasing amplitude greater than 20 kV NEMP, the microhardness values of light gray and dark gray BCC (I) solid solutions demonstrate an increase in comparison with the microhardness values of solid solutions of non-irradiated alloys, with an increase of 14.48% and 9.52%, respectively. The microhardness of the BCC (II) solid solution could not be determined due to the dispersibility of the phase.

– In alloys with 50 at.% Al and an amplitude of up to 20 kV NEMP, the microhardness values of the BCC (I) and BCC (II) solid solutions exhibited a respective increase of 53.5. At 6% and 44.85%, and then up to 40 kV NEMP, the microhardness of the solid solutions of BCC (I) remained practically unchanged, while that of BCC (II) decreased by 12.5%.

It can be posited that the observed increase in microhardness of light gray and dark gray BCC (I) solid solutions in alloys with 45 at. % aluminum is attributable to the rise in aluminum content, as evidenced by the increasing amplitude up to 40 kV. The maximum microhardness of BCC (I) and BCC (II) solid solutions in alloys with 50 at.% aluminum at 20 kV amplitudes is also attributable to the increase in aluminum and iron concentration.

Notwithstanding the observed increase in microhardness of light gray and dark gray BCC (I) solid solutions **(Fig. 7, *a*)**, the hardness of alloys with 45 at.% aluminum exhibits a pronounced dependence on NEMP amplitude, reaching a minimum value at NEMP irradiation with an amplitude of 30 kV **(Fig. 6, *b*)**.

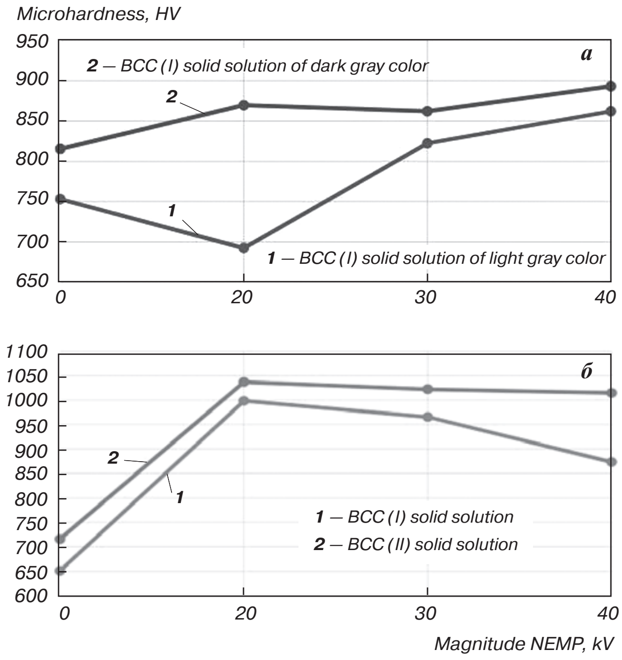

Fig. 7. Effect of NEMP amplitude on microhardness of solid solutions of synthesized alloy with 45 and 50 at.% Al:
a – 45 at.% Al, *b* – 50 at.% Al

The microhardness of BCC (I) and BCC (II) solid solutions in alloys with 50 at.% also exhibits a marked dependence, with a maximum observed at NEMP irradiation with an amplitude of 20 kV **(Fig. 6, *b*)**. Concurrently, the hardness of alloys undergoes a gradual change up to 30 kV, followed by a pronounced increase up to the NEMP amplitude of 40 kV. Therefore, there is a discrepancy between the correlation between the changes in microhardness of structural components (solid solutions) and the hardness of alloys. It is likely that the hardness of alloys is still influenced by the dispersion and amount of structural components and other factors.

Conclusions

1. The impact of NEMP amplitude (0, 20, 30, 40 kV) on the formation and liquation processes in high-entropy alloys of the Al*x* – Co – Cr – Fe – Ni system with varying aluminum content (45, 47, 50 at.%) synthesized via SHS metallurgy has been elucidated.

– An increase in NEMP amplitude has been observed to promote the refinement of structural constituents.

– In the presence of 45 at.% aluminum in alloys, BCC (I) solid solutions of light gray (type 1) and dark gray (type 2) colors do not crystallize and are not irradiated by NEMP with an amplitude of 30 kV. Additionally, at irradiation of melts by NEMP with an amplitude of 40 kV, a complex-alloyed BCC (II) solid solution is observed.

– As the aluminum content increases up to 50 at.%, in addition to BCC (I) of light gray and dark gray colors, a complex-alloyed solid solution, BCC (II), crystallizes in non- and NEMP-irradiated alloys.

The presence of BCC solid solutions was corroborated by *X*-ray diffraction analysis of alloys with varying aluminum content and amplitudes.

2. In alloys containing 45 atomic percent aluminum, the hardness values of the alloys exhibit minimal values (75 HRA) when subjected to NEMP irradiation at energies below 30 kV. In contrast, without irradiation, the hardness corresponds to 82 HRA. In alloys containing 50 atomic percent aluminum, the microhardness increases and reaches 90 HRA when subjected to NEMP irradiation, whereas without irradiation, it reaches 70 HRA.

3. In alloys containing 45 at.% aluminum and subjected to an increasing NEMP amplitude of up to 20 kV, the microhardness values of light gray and dark gray BCC (I) solid solutions exhibit an increase in comparison to the microhardness values of the non-irradiated alloy, with a percentage increase of 14.48% and 9.52%, respectively. The microhardness of light gray BCC (I) solid solutions is observed to be higher than that of dark gray solid solutions. In alloys with 50 at.% aluminum at 20 kV amplitude, the microhardness of BCC (I) and BCC (II) solid solutions increases by 53.56% and 44.85%, respectively, and then decreases by 2.5% up to 40 kV NEMP. The microhardness of BCC (I) solid solutions remains practically unchanged.

Acknowledgements

The research was carried out in the CPC "Applied Materials Science" of FSBOU HE "PNU" with the financial support of the Ministry of Science and Education of the Russian Federation within the framework of research work № FEME-2023-0009.

References

1. Cantor B., Chang I. T. H., Knight P., Vincent A. J. B. Microstructural development in equiatomic multicomponent alloys. *Materials Science and Engineering: A*. 2004. Vol. 375. pp. 213–218.

2. Yeh J. W., Chen S.-K., Lin S.-J., Gan J.-Y., Chin T.-S., Shun T.-T., Tsau C.-H., Chang S.-Y. Nanostructured High-Entropy Alloys with Multiple Principal Elements: Novel Alloy Design Concepts and Outcomes. *Advanced Engineering Materials*. 2004. Vol. 6, Iss. 5. pp. 299–303.

3. Tung C.-C., Yeh J.-W., Shun T.-T., Chen S.-K., Huang Y.-S., Chen H.-C. On the Elemental Effect of AlCoCrCuFeNi High-Entropy Alloy System. *Materials Letters*. 2007. Vol. 61, Iss. 1. pp. 1–5.

4. Senkov O. N., Wilks G. B., Scott J. M., Miracle D. B. Mechanical properties of $Nb_{25}Mo_{25}Ta_{25}W_{25}$ and $V_{20}Nb_{20}Mo_{20}Ta_{20}W_{20}$ refractory high entropy alloys. *Intermetallics*. 2011. Vol. 19, Iss. 5. pp. 698–706.

5. Wang Y. P., Li B. S., Ren M. X., Yang C., Fu H. Z. Microstructure and Compressive Properties of AlCrFeCoNi High Entropy Alloy. *Materials Science and Engineering:* A. 2008. Vol. 491, Iss. 1-2. pp. 154–158.

6. Sheng H. F., Gong M., Peng L. M. Microstructural Characterization and Mechanical Properties of an $Al_{0.5}CoCrFeCuNi$ High-Entropy Alloy in As-Cast and Heat-Treated/Quenched

Conditions. *Materials Science and Engineering: A*. 2013. Vol. 567. pp. 14–20.

7. Wang W.-R., Wang W.-L., Wang S.-C., Tsai Y.-C., Lai C.-H., Yeh J.-W. Effects of Al Addition on the Microstructure and Mechanical Property of Al_xCoCrFeNi High-Entropy Alloys. *Intermetallics*. 2012. Vol. 26. pp. 44–51.

8. Yen C.-C., Lu H.-N,, Tsai M.-H., Wu B.-W., Lo Y.-C., Wang C.-C., Chang S.-Y., Yen S.-K. Corrosion Mechanism of Annealed Equiatomic AlCoCrFeNi Tri-Phase High-Entropy Alloy in 0.5 M H_2SO_4 Aerated Aqueous Solution. *Corrosion Science*. 2019. Vol. 157. pp. 462–471.

9. Chuang M. H. et al. Microstructure and Wear Behavior of $Al_xCo_{1.5}CrFeNi_{1.5}Ti_y$ High-Entropy Alloys. *Acta Materialia*. 2011. Vol. 59, Iss. 16. pp. 6308–6317.

10. Li C., Li J. C., Zhao M., Jiang Q. Effect of Aluminum Contents on Microstructure and Properties of AlxCoCrFeNi Alloys. *Journal of Alloys and Compounds*. 2010. Vol. 504. pp. S515–S518.

11. Munitz A., Salhov S., Hayun S., Frage N. Heat Treatment Impacts the Micro-Structure and Mechanical Properties of AlCoCrFeNi High Entropy Alloy. *Journal of Alloys and Compounds*. 2016. Vol. 683. pp. 221–230.

12. Sourav A., Yebaji S., Thangaraju S. Structure-Property Relationships in Hot Forged Al_xCoCrFeNi High Entropy Alloys. *Materials Science and Engineering: A*. 2020. Vol. 793. 139877.

13. Garlapati M. M., Vaidya M., Karati A., Mishra S., Bhattacharya R., Murty B. S. Influence of Al Content on Thermal Stability of Nanocrystalline AlxCoCrFeNi High Entropy Alloys at Low and Intermediate Temperatures. *Advanced Powder Technology*. 2020. Vol. 31, Iss. 5. pp. 1985–1993.

14. Huang L., Yaoning Sun Y., Amar A. et al. Microstructure Evolution and Mechanical Properties of Al_xCoCrFeNi High-Entropy Alloys by Laser Melting Deposition. *Vacuum*. 2021. Vol. 183. 109875.

15. Shi Y., Mo J., Zhang F.-Y., Yang B., Liaw P. K., Zhao Y. In-Situ Visualization of Corrosion Behavior of Al_xCoCrFeNi High-Entropy Alloys During Electrochemical Polarization. *Journal of Alloys and Compounds*. 2020. Vol. 844. 156014.

16. Yang Y. C., Liu C., Lin C.-Y., Xia Z. Core Effect of Local Atomic Configuration and Design Principles in Al_xCoCrFeNi High-Entropy Alloys. *Scripta Materialia*. 2020. Vol. 178. pp. 181–186.

17. Joseph J., Haghdadi N., Shamlaye K., Hodgson P., Barnett M., Fabijanic D. The Sliding Wear Behaviour of CoCrFeMnNi and AlxCoCrFeNi High Entropy Alloys at Elevated Temperatures. *Wear*. 2019. Vol. 428-429. pp. 32–44.

18. Zhang G. J., Tian Q. W., Yin K. X., Niu S. Q., Wu M. H., Wang W. W., Wang Y. N., Huang J. C. Effect of Fe on Microstructure and Properties of $AlCoCrFe_xNi$ (x = 1.5, 2.5) High Entropy Alloy Coatings Prepared by Laser Cladding. *Intermetallics*. 2020. Vol. 119. 106722.

19. Kang M., Lim K. R., Won J. W., Na Y. S. Effect of Co Content on the Mechanical Properties of A2 and B2 Phases in $AlCo_x$CrFeNi High-Entropy Alloys. *Journal of Alloys and Compounds*. 2018. Vol. 769. pp. 808–812.

20. Qin G., Xue W., Fan C., Chen R., Wang L., Su Y., Ding H., Guo J. Effect of Co Content on Phase Formation and Mechanical Properties of $(AlCoCrFeNi)_{100-x}Co_x$ High-Entropy Alloys. *Materials Science and Engineering: A*. 2018. Vol. 710. pp. 200–205.

21. Tang Z., Senkov O. N., Parish C. M. et al. Tensile Ductility of an AlCoCrFeNi Multi-Phase High-Entropy Alloy Through Hot Isostatic Pressing (HIP) and Homogenization. *Materials Science and Engineering: A*. 2015. Vol. 647. pp. 229–240.

22. Muthupandi G., Lim K. R., Na Y.-S., Park J., Lee D., Kim H., Park S., Choi Y. S. Pile-Up and Sink-In Nanoindentation Behaviors in AlCoCrFeNi Multi-Phase High Entropy Alloy. *Materials Science and Engineering: A*. 2017. Vol. 696. pp. 146–154.

23. Lim K. R., Lee K. S., Lee J. S., Kim J. Y., Chang H. C., Na Y. S. Dual-Phase High-Entropy Alloys for High-Temperature Structural Applications. *Journal of Alloys and Compounds*. 2017. Vol. 728. pp. 1235–1238.

24. Zhang C., Diao H., Gao M. C., Tang Z., Poplawsky J. D., Liaw P. K. Understanding Phase Stability of Al – Co – Cr – Fe – Ni High Entropy Alloys. *Materials & Design*. 2016.Vol. 109. pp. 425–433.

25. Deev V. B., Ri E. Kh., Prusov E. S., Ermakov M. A., Goncharov A. V. Modification of Al – Mg – Si Casting Aluminum Alloys by Liquid Phase Processing with Nanosecond ElectromagneticPulses. *Izvestiya Vuzov. Tsvetnaya Metallurgiya*. 2021. Iss. 4. pp. 32–41.

26. Andersson J.-O., Helander T., Höglund L., Shi P., Sundman B. Thermo-Calc & DICTRA, Computational Tools for Materials Science. *Calphad*. 2002. Vol. 26, Iss. 2. pp. 273–312.

NFM